Journal of Materials Chemistry C

PAPER

View Article Online
View Journal | View Issue

Cite this: J. Mater. Chem. C, 2015, 3, 623

Poly(ionic liquid)-based monodisperse microgels as a unique platform for producing functional materials†

Jiecheng Cui,‡ Ning Gao,‡ Jian Li, Chen Wang, Hui Wang, Meimei Zhou, Meng Zhang and Guangtao Li*

Received 31st October 2014
Accepted 11th November 2014

DOI: 10.1039/c4tc02487g

www.rsc.org/MaterialsC

In this work, we report the microfluidic preparation of monodisperse imidazolium-based poly(ionic liquid) (PIL) microgels with a controlled size and morphology, and show that the imidazolium units in the microgel network can be exploited as reactive sites to efficiently access desired functional materials by a simple counteranion-exchange or conversion reaction. Moreover, based on the counteranion-exchange reaction, spatio-temporal engineering of the surface of the PIL microgels could also be realized, and a new and simple strategy for the fabrication of diverse anisotropic microgels (patchy particles) with great flexibility was developed. In addition, by exploiting the convenient generation of carbene units from the imidazolium moieties, as well as the carbonizable feature of PIL, the prepared PIL microgels could be further converted into stable carbene spheres and monodisperse carbon particles. All the results show that these monodisperse PIL-based microgels can serve as a very useful platform for facilely accessing various functional materials.

Introduction

Polymer microgels are micrometer-sized particles, which have a three-dimensional network structure and are inflated with a solvent.[1] Due to their unique structural features, microgels have attracted increasing attention over the past few years and have been exploited for various applications in drug delivery, chemical sensing, separation and purification techniques, the fabrication of photonic crystals, and catalysis for organic and inorganic synthesis.[2] Recently, due to their promising application as smart nanoreactors, the introduction of metal nanoparticles into polymer microgels to produce hybrid microgels has attracted considerable attention.[3] However, to achieve microgels with the desired function and sufficient mechanical strength, traditionally each fabrication method is strongly dependent on the screening and on an arduous synthesis of a functional monomer, as well as on optimization of the polymerization conditions. Especially in the case of sensitive functional moieties (*e.g.*, bioactive units) incompatible with the conventional thermal- or photo-induced polymerization process, the traditional polymerization methods are inappropriate or have difficultly in fabricating the corresponding microgels. Thereby, developing a new strategy to efficiently access monodisperse functional microgels with controlled sizes and morphologies is highly desirable.

Ionic liquids (ILs), a class of salts composed of discrete organic cations and anions, exhibit a series of unique properties, including negligible vapor pressure, non-flammability, high ionic conductivity, a wide electrochemical window, and good chemical and thermal stability.[4] Importantly, such favorable properties can be individually manipulated through modulating the combination of cations and anions, thus providing unprecedented tunability.[5] Thereby, these distinct physiochemical properties and features make ILs ideal candidates for the design and development of functional materials and chemical systems. Some studies have demonstrated the applications of ionic liquids or their polymers (PILs) in the fabrication of functional materials through the counteranion-exchange reaction.[6,7] However, few works have been reported on multifunctional microgels and patchy microparticles, which presents an exciting new research area and have attracted an increasing attention due to their strongly anisotropic and directional interactions.[8] In this respect, there are still some challenges needed to be faced. More importantly, the properties of ionic liquids are actually much more than just the counteranion-exchange feature. Especially, in the case of imidazolium-based PILs, the imidazolium moiety is not only a "reactive site" for counteranion exchange, but it can also serve as carbene and carbon precursors.[4,9] It is conceivable that the exploitation of these unique properties of the imidazolium moiety could open

Department of Chemistry, Key Lab of Organic Optoelectronics & Molecular Engineering, Tsinghua University, Beijing 100084, P. R. China. E-mail: LGT@mail.tsinghua.edu.cn; Fax: +86 10-6279-2905

† Electronic supplementary information (ESI) available. See DOI: 10.1039/c4tc02487g

‡ These authors contribute equally to this paper.

up an efficient avenue to access various functional microgels and materials from PIL-based microgels.

Inspired by the unique properties of ILs, herein, we report on the microfluidic synthesis of monodisperse imidazolium-based PIL microgels, and show that the imidazolium units in the resultant polymer network indeed can be exploited as functional sites to efficiently access desired functional materials by not only simple counteranion exchange, but also by the conversion reaction. As demonstration, three types of isotropic functional particles, including metal–polymer hybrid particles, conductive composite particles, and catalytic particles, were first evolved from the prepared PIL microgels. More importantly, based on the "task-specific" concept of ILs,[7] the surface of the PIL microgels could be spatio-temporally engineered to afford multifunctional, as well as patchy microparticles. Thus, a new and efficient strategy was developed to realize the fabrication of multifunctional patchy microparticles with great flexibility. Moreover, due to the convenient generation of carbene units from the imidazolium moieties, as well as the carbonizable feature of PIL, the prepared PIL microgels could be further converted into stable carbene spheres and monodisperse carbon particles. These monodisperse PIL-based microgels can serve as a useful platform for facilely accessing various functional materials (Scheme 1).

Results and discussion

Synthesis of the monodisperse PIL-based microgels

The microfluidic synthesis of microgel particles begins with the emulsification of a precursor solution in an immiscible liquid. The resulting particle dimensions and their uniformity are predetermined in the microfluidic emulsification stage. In previous works,[10] it was verified that the diameter of the formed precursor droplets (D_d) (and hence, the corresponding solid particles) is sensitive to a number of preparation parameters, including the caliber of the glass capillary microchannel (D_g), the viscosity of the continuous phase (u_c) and dispersed phase (u_d), the flow velocity of the continuous phase (v_c) and dispersed phase (v_d), and the interfacial tensions between the continuous and dispersed phases. Recently, C. Serra and coworkers established that the diameter of the resulting droplets in microfluidic emulsions is a function of the channel dimensions, the flow rates, viscosities, and the interfacial tensions between the continuous and dispersed phases, as follows:[11]

$$D_d/D_g = K(Ca_c/Ca_d)^M$$

where K and M are constant, Ca_c and Ca_d are the capillary number for the continuous phase and the dispersed phase, and $Ca_c = u_c v_c/\gamma$, $Ca_d = u_d v_d/\gamma$, and γ is the interfacial tension. Moreover, for a given emulsion system in a microfluidic device, the dimensions of the formed particles can be controlled by tuning the flow rates of the continuous and dispersed phases.

In the present work, a co-flowing microfluidic device was employed to produce droplets with a narrow size distribution, as shown in Scheme S1.† Poly(dimethylsiloxane) with surfactants was used as the continuous oil phase, and the dispersed phase was an aqueous solution of 1-butyl-3-vinylimidazolium as the monomer and 1,6-di(3-vinylimidazolium) hexane as the cross-linker (Scheme 1). As previously reported in the literature,[11] the diameter of the droplets increases when the flow rate of the dispersed phase increases or when the flow rate of the continuous phase decreases. In fact, because the velocity (v_d) of the dispersed phase is considerably lower compared to the continuous phase, the control of the continuous phase velocity is found to be a more practically useful means for generating droplets with a good controlled bead size and high repeatability. Thus, in this work, the control of the flow rates of the continuous and dispersed phases was employed to realize the formation of microgel particles with different sizes. Microgels of 467 μm were obtained when $v_d = 0.5$ mL h^{-1} and $v_c = 25$ mL h^{-1} were used (Fig. 1a). As mentioned above, the regulation of the flow rate of the continuous phase provides more effective control over the size of the resulting microgel particles. When the flow rate of the continuous phase was increased from 25 mL

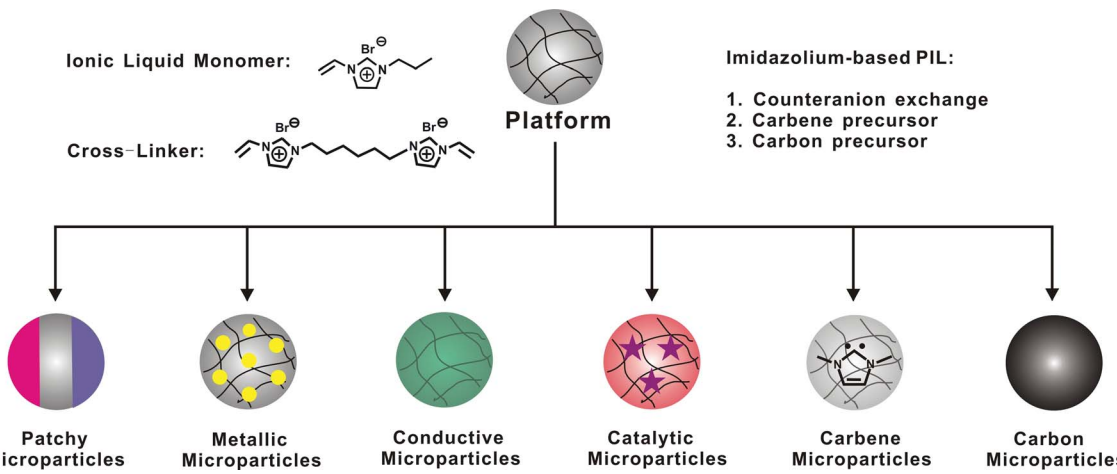

Scheme 1 Poly(ionic liquid)-based monodispersed microparticles as a unique platform for producing functional materials, including patchy particles, metal-containing microgels, conductive composite particles, catalytic particles, carbene particles, and carbon particles.

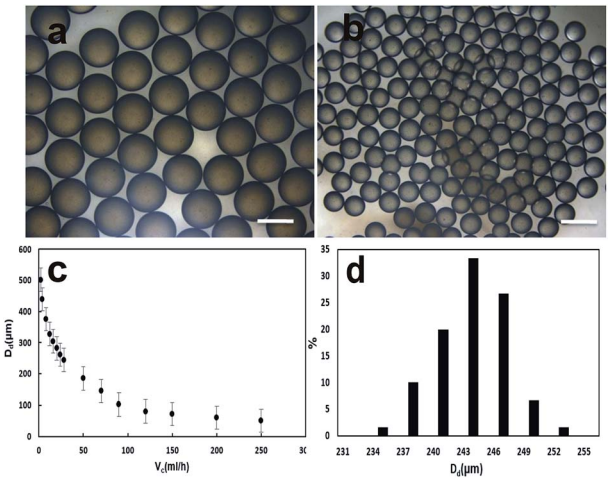

Fig. 1 Optical images of the fabricated PIL microgels with a diameter of 467 μm (a) and 233 μm (b). The scale bar is 450 μm; (c) relationship between the diameter of the droplets D_d and the flow velocity of the continuous phase (v_c) under the conditions: $v_d = 0.5$ mL h^{-1}, $D_g = 120$ μm and 50 cSt silicone oil as the continuous phase; (d) size distribution of microgels, the mean diameter and the coefficient of variation of the formed microgels (244 μm).

h^{-1} to 100 mL h^{-1}, microgels with an obvious smaller diameter (233 μm) were obtained (Fig. 1b). Fig. 1c shows the correlation between the flow velocity of the continuous phase (v_c) and the sizes of the formed droplets (D_d) under conditions as follows: v_d = 0.5 mL h^{-1}, D_g = 120 μm and 50 cSt silicone oil as the continuous phase. Clearly, it can be seen that with an increased flow velocity of the continuous phase, the diameter of the formed droplets gradually decreases. Certainly, the viscosity of the continuous phase also has an obvious effect on the droplet size. Generally, a high viscosity of the continuous phase leads to a smaller particle diameter, due to the relative increase in the shear force exerted on the dispersed phase by the continuous phase over the interfacial force. In our case, the dispersion of the particle sizes is quite low (Fig. 1d). Under optimized conditions, the microfluidic generation of polymer particles with a polydispersity below 1–2% is possible. These results indicate that using a simple microfluidic system, monodisperse PIL microgels with controlled sizes could be facilely fabricated. In our case, the value of M in the above equation was determined to be −0.27 by analyzing the parameter such as D_d, D_g, v_c, v_d, u_c, and u_d in the size control experiments of the microgels.

As expected, the prepared PIL particles exhibit the characteristic features of microgels. The original PIL particles (with Br^- as the counteranion) exhibited considerable swelling in water or water solution. Upon exposure to air atmosphere, the swollen PIL particles gradually became smaller with the loss of water molecules (Fig. 2a) and their size dramatically changed from a swollen to dried state, for example from 850 μm to 230 μm. The swelling and deswelling process is completely reversible. Moreover, it is found that upon exposure to different organic solvents, the prepared PIL particles exhibit different swelling (Fig. 2b).

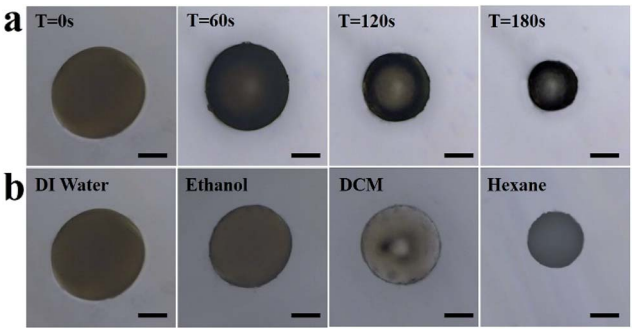

Fig. 2 (a) Size evolution of the swollen PIL microgels exposed to the air (b). Swelling of the prepared PIL particles exposed to different organic solvents. Scale bar is 100 μm.

Counteranion-exchange behavior of the PIL microgels

As mentioned in the introduction, one of the most attractive features of ILs is that their physicochemical properties and functionality can be easily tailored by simple counteranion exchange. Thus, the counteranion-exchange behavior of the prepared PIL microgels (with Br^- as the counteranion) was first examined using three salts, namely, sodium tetrafluoroborate ($NaBF_4$), lithium bis(trifluoromethane sulfonimide) ($LiTf_2N$), and sodium hexafluorophosphate ($NaPF_6$) (Scheme S2†). As expected, upon exposure of the fabricated microgels to an aqueous solution of the chosen salts, a gradual shrinkage of their sizes was observed, indicative of the occurrence of the counteranion-exchange reaction. With the displacement of Br^- by hydrophobic anions, the prepared PIL microgels became smaller. The more hydrophobic is the used counteranion, the smaller the microgels became (Fig. 3). The counteranion-exchange reaction seems relatively fast and took about two hours for the used microgels. Indeed, the FTIR analysis confirmed the occurrence of the anion exchange and the

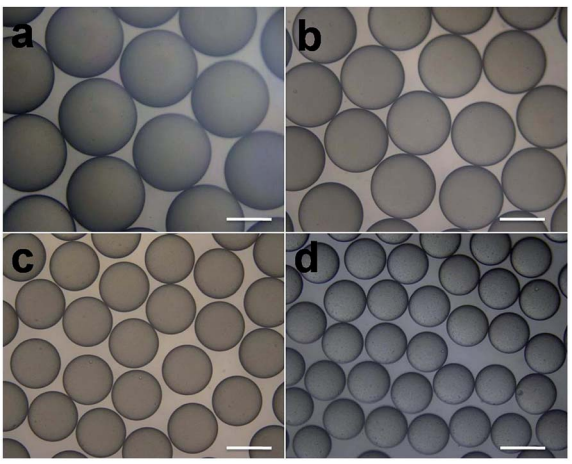

Fig. 3 Optical images of the PIL microgels with different counteranions: (a) microgels with Br^- as counteranion (diameter: 370 μm); (b) microgels with BF_4^- as counteranion (diameter: 305 μm); (c) microgels with PF_6^- as counteranion (diameter: 236 μm); (d) microgels with Tf_2N^- as counteranion (diameter: 189 μm). The scale bar is 200 μm.

existence of the chosen anions. Fig. S1 in the ESI† shows the comparison of the FTIR spectra of the PIL microgel particles before and after exposure to different anion aqueous solutions. It is clearly seen that the characteristic absorption bands of the used anions were detected at 1083 cm^{-1} (BF_4^-), 838 cm^{-1} (PF_6^-), and 1356 cm^{-1} (Tf_2N^-).[12]

To visualize the anion-exchange process, in this work, three typical dye molecules (SPADNS, 9,10-anthraquinone-2-sulfonic acid sodium salt, and indigo carmine in Scheme S2†) were employed to further confirm the feasibility of the introduction of a specific function in the PIL microgels by an anion-exchange reaction. Similarly, the prepared PIL microgels (with Br^- as the counteranion) were soaked in aqueous solution of the corresponding dye molecule at room temperature for 12 h. After being filtered off, the treated PIL microgels were thoroughly washed to remove the physically trapped dye molecules until no coloration was observed in the washing solution. As shown in Fig. 4, the treated PIL microgels, exhibiting a clear color throughout the microgels, display a different appearance from the original PIL microgels, which do not exhibit any optical property (Fig. 1). Fig. 5 shows the UV-vis spectra of the used dye molecules and the PIL microgels before and after the counter-anion-exchange treatment. Obviously, by simple anion-exchange the optical properties of the functional anions were correctly introduced into the PIL microgels. These results clearly indicate that the counteranion-exchange property of the ionic-liquid units inside the PIL microgels is still retained, and that the functional groups could be facilely introduced into the prepared microgels *via* an anion-exchange reaction.

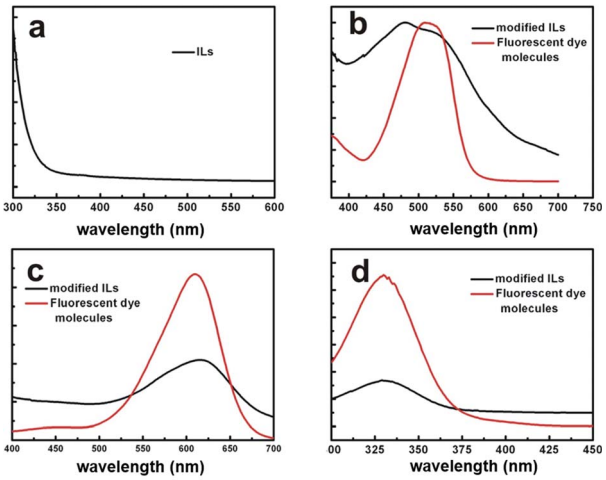

Fig. 5 UV/vis spectra of the fabricated PIL microgels before and after the treatment with an aqueous solution of different dye molecules: (a) original PIL microgel; (b) treated with SSPADNS; (c) treated with indigo carmine; (d) treated with 9,10-anthraquinone-2-sulfonic acid sodium salt. For comparison the UV/vis spectra of the used dye molecules are also includes, respectively.

Preparation of patchy microgels or particles through spatio-temporal engineering of the surface of the PIL microgels

Compared to the monofunctional microgel particles described above, multifunctional microgels, as well as anisotropic patchy particles, are another more interesting class of particles that exhibit completely different properties and that hold promise for use in numerous applications.[13] In this respect, the surface of PIL microgels were designed by spatio-temporal engineering to achieve multifunctional microparticles, as well as patchy particles. Due to the counteranion-exchange capability of ionic liquids, the PIL also show great flexibility in surface chemistry engineering, and allow for producing various multifunctional anisotropic structures. Using a "sandwich" microcontact printing (μCP) (Scheme S3†) method,[14] the PIL microgels with A–B, A–B–A, or A–B–C patchy structures were easily accessible (Fig. 6). In this work, for visual inspection, two fluorescent counteranions (Indigo carmine and SPADNS) were used as a chemical "ink" and the PDMS elastomer was utilized as a

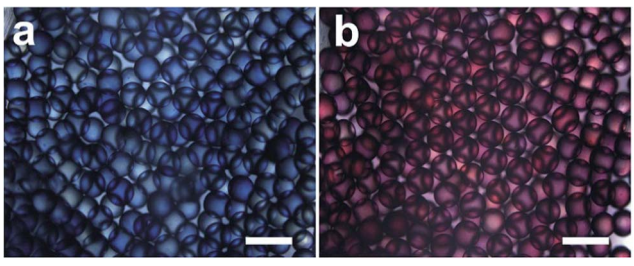

Fig. 4 Optical images of the fabricated PIL microgels after the exposure to indigo carmine (a), and SPADNS (b) aqueous solution, respectively. The scale bar is 500 μm.

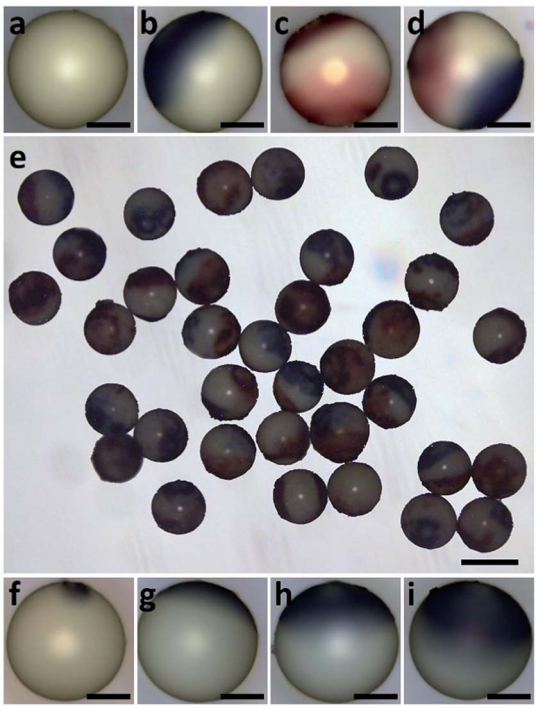

Fig. 6 Optical images of the original PIL microgel (a) and the derivated patchy particles with an A–B structure (b), with an A–B–A structure (c) with an A–B–C structure (d and e); the microgels with tunable patchy size (f–i). The scale bar is 100 μm (a–d and f–i) and 300 μm (e).

stamp. It was found that the printing process in our case proceeded very fast at room temperature. It took only several minutes to transfer the "ink" to the PIL microgels *via* counteranion exchange exclusively in the area of contact. The contact time and pressure could be used to tune the size of the formed patchy microgels (Fig. 6f–i). Due to the unlimited combination of cations and anions,[5] although only fluorescent anisotropic PIL microgels were fabricated, principally unlimited PIL patchy particles could be easily accessible through a simple counteranion-exchange reaction, including biomolecule-binding patchy particles and magnetic patchy particles. Compared to the numerous developed approaches,[13] the spatio-temporally engineered surface strategy described here is simple and versatile, offering a broad design space for fabricating desired multifunctional materials (patchy microparticles) under mild conditions.

Fabrication of various functional microgels using PIL microgels

On the basis of the concept of "task-specific" ionic liquids,[7] a variety of functional groups as anions can be readily introduced into the PIL-IOMS by a simple anion-exchange reaction, leading to new microgels or spheres with desired functions. Thus, the immobilization of metal nanoparticles in microgels through the counteranion-exchange reaction followed by reduction of the incorporated metallic complex is possible. Recently, the uniform and homogenous metal–polymer hybrid microgels have fascinated scientists, due to their potential applications in chemical sensing or as nanoreactors. Under this consideration, in our work, Au–PIL hybrid microgels were synthetized by introducing a precursor $AuCl_4^-$ anion into the PIL microgels *via* counteranion exchange and subsequent reduction using $NaBH_4$ as a reducing agent (Scheme S4†). Fig. 7a and b shows the optical and TEM images of the prepared Au–PIL hybrid microgels. Compared to the original PIL microgels (with Br^- as the anion), the resultant microgels show considerable shrinking of their particle size and exhibit a purple color, indicative of the formation of gold nanoparticles (Fig. 7a). Under TEM observation, a large number of gold dark dots with a diameter of about 20 nm were detected to be homogeneously distributed inside the PIL microgels (Fig. 2b). Fig. S2 and S3† show the TGA and EDX spectra of the prepared Au–PIL hybrid microgels. The TGA measurement demonstrates that 2 wt% Au nanoparticles were immobilized into the PIL microgels. Moreover, the content of the Au nanoparticles can be up to 6 wt% by adjusting the amount of $AuCl_4^-$ introduced during the counteranion-exchange reaction. Interestingly, it was found that the trapped Au nanoparticles in the PIL gels display a remarkable stability and that no leakage or aggregation of the Au nanoparticles was detected with the prolonged storage of the hybrid microgels in water. Recently, numerous works have reported the similar phenomenon that some ionic liquids, especially imidazolium-based ionic liquids, can hold stable suspensions of metallic nanoparticles without additional surface-active agents.[15] Using XPS and Raman analysis, several studies suggest that in the case of imidazolium-based ionic liquids, a strong interaction between metal particles with positively charged imidazolium rings is present, which is responsible for the solvation and stability of the nanoparticles in ionic liquids. On the basis of these results, we believe that the same stabilization mechanism could be used to explain the observed phenomenon in our case. Additionally, after the displacement of Br^- by $AuCl_4^-$ anions, followed by reduction using $NaBH_4$, (Scheme S4†), it was found that the resulting Au-containing microparticles have a smaller size compared to the original microgels (with Br^- as the anion). The exact reason for this phenomenon is still not clear. Probably, the strong interaction between gold particles with IL moieties reduces the size of the resulting composite particles.

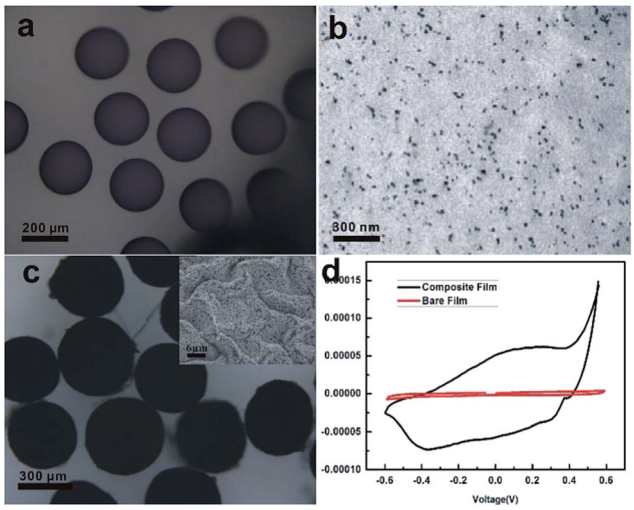

Fig. 7 (a) Optical image of the microgels containing Au nanoparticles; (b) TEM image of the microgels containing Au nanoparticles; (c) optical image of the conductive microgels; inset is the SEM image of the prepared conductive particles, (d) cyclic voltammograms of the original PIL microgel and the resulting composite conductive particles.

Interestingly, we found that the $AuCl_4^-$ anions incorporated into PIL microgels could also serve as reducing agents to produce uniform conducting polymer spheres when the PIL microgels were exposed to the solution of pyrrole. Fig. 7c displays the optical image of the resulting conductive hybrid particles, which shows a quit different morphology from the original microgels. In particular, under SEM observation, the obtained conducting polymer (polypyrrole) microparticles show a typical granular morphology (Inset in Fig. 7c), and the polypyrrole coating on the surface is very evident. Importantly, electrochemical analysis of the formed particles provide direct evidence for the formation of conductive polypyrrole inside the particles. As shown in Fig. 7d, the redox behavior of the polypyrrole composite spheres was investigated by cyclic voltammetry. Compared to the original microgels, which do not exhibit any electrochemical activity in the range from −0.6 V to 0.6 V, the resulting composite spheres show the characteristic redox feature of polypyrrole.

As a further demonstration, polyoxometalates (POMs) were chosen as task-specific building blocks and introduced into the PIL microgels. POMs are a family of anionic, inorganic metal oxides, and exhibit a wide range of topologies and a very rich

redox chemistry that provides the basis for their high catalytic activity in oxidation reactions.[16] The combination of organic cations of the PIL microgels with POM anions could not only lead to the formation of recoverable catalysts, but also the microgels with electrochemical activity are obtained (Fig. 8). In this study, the dinuclear peroxotungstate $[\{W(=O)(O_2)_2(H_2O)\}_2(\mu\text{-}O)]^{2-}$[17] was used as a catalytic anion, due to its high efficiency of H_2O_2 utilization and high selectivity to the epoxides.[16] The incorporation of the PIL microgels with peroxotungstate was simply achieved through the exposure of the PIL microgels to an aqueous solution of the potassium salt of peroxotungstate at RT for 12 h. FTIR measurements confirmed the correct loading of peroxotungstate active species into the interior of the PIL microgels. Compared to the FTIR spectrum of the original PIL microgels, the characteristic bands[18] of peroxotungstate at 1080 cm^{-1}, 978 cm^{-1}, 895 cm^{-1}, and 812 cm^{-1} were detected in the treated samples (POM@PIL) (Fig. 8a). The catalytic performance of POM@PIL microgels was evaluated using the oxidation reaction of olefins. Consequently, POM@PIL microgels were dispersed in an acetonitrile solution of cyclooctene with hydrogen peroxide as an eco-friendly oxidant. The oxidation reaction was carried out at 333 K with stirring. At given time intervals of reaction, the product and yield were determined by GC/MS analysis. It was found that the POM@PIL microgels exhibited excellent catalytic activity. After 5 h, 93% of cyclooctene were converted into the corresponding epoxides. The above results indicate that the observed catalysis indeed originates from the ionic bonded peroxotungstate species, and that the catalysis of the POM@PIL microgels is truly heterogeneous in nature. As a control experiment, the same reaction mixture only without POM@PIL microgels was stirred at 333 K for 5 h. As expected, the conversion was as low as 1.77%. Moreover, the catalytic property of the POMs-incorporated microgels was compared with that of pure POMs under the same conditions. It was found that 98% of cyclooctene was converted into the corresponding epoxides using pure POMs. This result indicates that the catalytic performance of the POMs remain nearly unchanged after their incorporation into microgels.

Fabrication of uniform carbene spheres from PIL microgels

Since the first isolation and characterization of stable N-heterocyclic carbenes (NHCs) by Arduengo in 1991, these compounds have attracted significant interest in various fields of chemistry.[19] As molecules with divalent carbon atoms, NHCs are not only of theoretical interest but also of practical relevance as versatile ligands and effective organocatalysts. In our work, we found that the PIL microgels produced from the imidazolium-based IL mononer could be readily transformed to stable N-heterocyclic carbine microspheres by deprotonation of the imidazolium moieties with sodium hydride in tetrahydrofuran in the presence of a catalytic amount of dimethyl sulfoxide (Fig. 9a).[19] Because of their high basicity, N-heterocyclic carbenes can rapidly react with CO_2 to afford zwitterionic adducts (designated as NHC–CO_2), even at very low CO_2 concentrations. Indeed, it is found that the resultant carbene spheres can be used as a highly efficient adsorbent for the reversible fixation-release of CO_2. Fig. 9c shows the FTIR spectra of the microspheres before and after the reaction with CO_2. The appearance of the asymmetric $\nu(CO_2)$ vibrations of the NHC–CO_2 adduct at 1649 cm^{-1} confirmed the presence of the NHC moieties in the microspheres.[20] As expected, the produced carbene microspheres show an excellent catalytic effect for transesterification and for acylation reactions. In our study, a simple transesterification of benzyl alcohol and vinyl acetate in tetrahydrofuran was performed in the presence of the carbene spheres and under a nitrogen atmosphere (Fig. 9b). Consequently, monodisperse carbene spheres were dispersed in a tetrahydrofuran solution of benzyl alcohol and vinyl acetate. The reaction was carried out at 298 K with stirring. At given time intervals of reaction, the product and yield were determined by GC/MS analysis. After 10 min, the reactants were quantitatively converted into product. This indicated that the carbene spheres

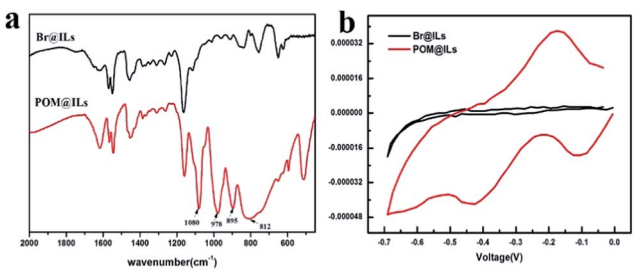

Fig. 8 (a) FT-IR spectra of the fabricated PIL microgels before and after treatment with an aqueous solution of peroxotungstate; (b) cyclic voltammograms of the original PIL microgels before and after the counteranion exchange with POM.

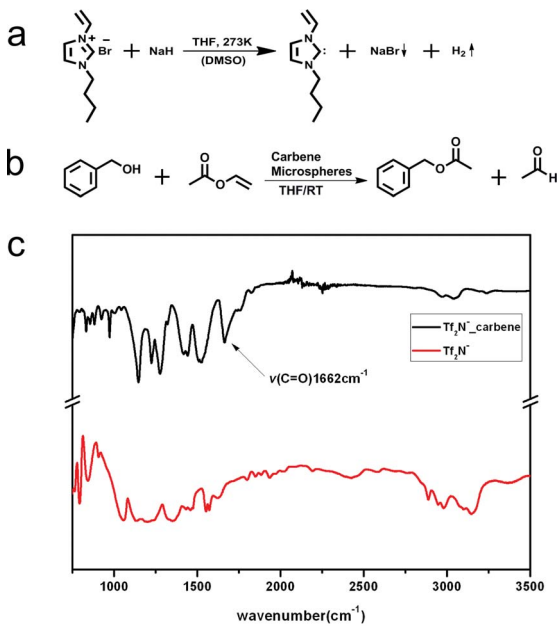

Fig. 9 Model reaction for synthesis of crabene (a) and the evaluation of the catalytic capability of the carbene microspheres (b); (c) FTIR spectra of the prepared carbene microspheres before and after the reaction with CO_2.

exhibited excellent catalytic activity. In contrast, the same reaction did not occur without the assistance of the carbene spheres. Probably due to the steric hindrance offered by the polymeric network, the obtained carbene microspheres show remarkable stability and could serve as recoverable catalysts. As a control experiment, the catalytic property of pure NHCs was also studied under the same conditions. It was found that the catalytic performance of the NHCs nearly remain unchanged after their incorporation into microgels.

Fabrication of uniform carbon spheres using PIL microgels

The unique features of ionic liquids mentioned in the introduction section have led to the wide use of ILs in many areas, for instance, as materials for fabricating different types of functional materials through counteranion exchange, as solvents for organic and inorganic synthesis, and as electrolytes for energy applications. In an effort to extend new applications, ionic liquids and their polymers have been found to be excellent precursors for producing functional carbon materials.[4b] Fig. 10 shows the optical image of carbon microspheres produced from carbonizing the PIL microgels at 1073 K under a N_2 atmosphere. Obviously, all the carbon spheres preserve a spherical morphology and have a narrow size distribution. However, considerable shrinkage of the particle size occurred during the carbonization process, and thus the diameter of the resultant carbon particles is considerably smaller compared to the parent particles. For example, the carbonization of the PIL microgels with a diameter of 420 μm afforded 80 μm carbon spheres. Nevertheless, this result indicates that different monodisperse carbon particles can be readily fabricated by choosing PIL microgels with different particle sizes. The cross-linked polymer structures and surface tension of the microgels are the principal reason for the retention of the spherical morphology under high-temperature annealing.

A Raman spectrum of the obtained carbon spheres reveals two distinct peaks at 1350 cm^{-1} and 1580 cm^{-1} (Fig. 10b), confirming the presence of amorphous and graphitic carbon domains.[21] The 1580 cm^{-1} band is associated with a graphitic carbon with a sp^2 electronic configuration. The band at 1350 cm^{-1} arises from polycrystalline graphite, and can be attributed to diamond-like carbon atoms with a sp^3 configuration. Earlier work in our laboratory suggested that the area ratio of Asp^3 to Asp^2 decreased with increasing the carbonization temperature.[22] Thus, the carbonization of the PIL microgels at higher temperatures can lead to further graphitized structures.

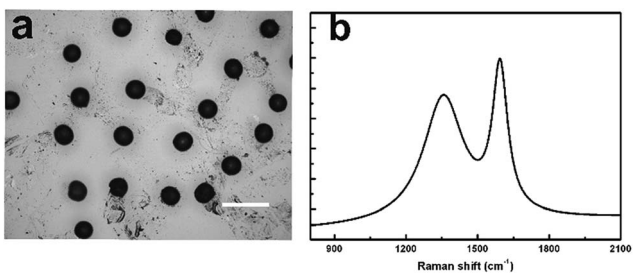

Fig. 10 (a) Optical image of the resulting carbon spheres; (b) Raman spectrum of the resulting carbon spheres. The scale is 200 μm.

Conclusions

In summary, using a microfluidic approach, we successfully produced monodisperse poly(ionic liquid) microgels with controlled size and morphology. On the basis of the utilization of the unique properties of poly(ionic liquid), such as spatio-temporal engineering of the microgels' surface through a counteranion-exchange reaction, the imidazolium-based conversion reaction, as well as the carbonizable feature it was found that the poly(ionic liquid) microgels could be easily evolved for conveniently fabricating functional materials with a variety of potential applications. Due to the unlimited combination of cations and anions, principally unlimited PIL multifunctional materials, as well as anisotropic patchy particles are easily accessible. The imidazolium-based conversion reaction of poly(ionic liquid) provides another opportunity to construct unique carbene microspheres with remarkable stability, which shows promising catalytic applications as heterogeneous catalysts. Additionally, the carbonizable feature of poly(ionic liquid) allows for efficiently producing monodisperse carbon particles. All the obtained results clearly indicate that, as a unique platform, these poly (ionic liquid) microgels could provide tremendous opportunities, principally unlimited possibilities for facilely accessing various functional materials.

Experimental section

Chemicals

All the solvents and chemicals are of reagent quality and were used without further purification unless otherwise specifically explained. 1-Vinylimidazole and 1-bromobutane 1,6-dibromohexane were purchased from Alfa and used as received. Silicone oil (20 cSt, 50 cSt) and 2,2-azobis(2-methylpropion-amidine) dihydrochloride (AIBA) as the photoinitiator were purchased from Aldrich. Polydimethylsiloxane (KF-96 10 cSt) was obtained from Shin-Etsu Chemical, Japan. Silicone oil and span80 were brought from Yunuo Chemicals Ltd, China.

Instrumentation

^1H NMR spectra were obtained using a JEOLJNMECS 300NMR spectrometer. UV-vis spectra were obtained on a PerkinElmer Lambda35 spectrometer. The photopolymerization was carried out under UV light. The microstructures of the beads were characterized by a scanning electron microscopy (SEM, HITACHI, S-300N). Images of the beads were taken using an optical microscope (OLYMPUS BXFM) equipped with a CCD camera. The microfluidic devices were homemade by glass capillary tubes with an inner diameter of 75 μm and an outer diameter of 200 μm and a T-junction. The monomer dispersed phase and oil continuous phase were delivered by syringe pumps. The dispersed phase was injected *via* a glass capillary tube positioned along the main axis of the T-junction. The continuous

phase was injected perpendicular to the main axis of the T-junction.

Synthesis of the ionic liquid monomers

The ionic liquid monomer, 1-butyl-3-vinylimidazolium bromide was synthesized according to the literature.[23] 1-Vinylimidazole (6.00 g, 64 mmol) was mixed with 1-bromobutane (10.5 g, 76.8 mmol), and the mixture was vigorously stirred at 343 K. After 3 h reaction, the residual 1-bromobutane was removed under vacuum at 333 K to afford a yellow solid. The dicationic 1,6-di(3-vinylimidazolium)hexane bromide as cross-linker was synthesized as follows: a mixture of 2 molar equivalents of 1-vinylimidazole and 1 molar equivalent of 1,6-dibromohexane was stirred at room temperature until the IL solidified. Then, the bromide salt was dissolved in water, and the mixture was washed three times with ethyl acetate to remove impurities. The last residue was evaporated in vacuum to ensure complete dryness. ^{1}H NMR (300 MHz, DMSO-d6, δ): 9.56(s, 2H, –NCHN–), 8.22(s, 2H, –NCHC–), 7.95(s, 2H, –CCHN–), 7.31(m, 2H, –CH=CH_2), 5.97(dd, $J = 2.4$ Hz, $J = 15.8$ Hz, 2H, –HCH=CHN–), 5.44(dd, $J = 2.07$ Hz, $J = 6.54$ Hz, 2H, –HCH=CHN–), 4.21(t, $J = 7.2$ Hz, 4H, –NCH_2CH_2), 1.84(t, $J = 6.87$ Hz, 4H, $NCH_2CH_2CH_2$), 1.31(m, 4H, –$CH_2CH_2CH_2$–).

Preparation of monodisperse PIL microgels

1.2 g IL monomer and 0.4 g cross-linker were dissolved in 400 μL water containing 2,2-azobis(2-methylpropion-amidine) dihydrochloride (AIBA) as photoinitiator. To produce monodisperse PIL microgels, the homemade microcapillary devices were used as shown in Scheme 1. The oil phases was poly(polydimethylsiloxane) with span80 as the stabilizer. We pumped the aqueous solution of ILs and oil phases into the inner and outer capillaries at volumetric flow rates of about 0.5 mL h^{-1} and 50 mL h^{-1}, respectively. Then, the aqueous flow was broken into droplets by the oil flow at the needle tip. The generated droplets were solidified by photopolymerization under UV exposure of less than 1 min and the resulting PIL microgels were taken into the collection container filled with the oil by the oil flow. The generated PIL microgels were rinsed several times with hexane, and deionized water, to remove the silicone oil and the residual surfactant.

Monodisperse PIL microgels as a platform to produce functional materials

(A) Patchy microgels. The patchy PIL microgels were fabricated with a versatile strategy using a "sandwich" contact printing (μCP) method. The PDMS stamps were loaded with a few drops of the respective chemical ink solution (10^{-8} mM, aqueous solution of fluorescent dye molecules) and the excess ink solution was removed under a stream of argon. Then, the PIL microgels were loaded onto the stamp and a second stamp loaded with the second ink (like the first one) was placed on top using a press. The samples were left to react at room temperature. It took several minutes to transfer the "ink" to the PIL microgels *via* a counteranion-exchange only in the area of contact.

(B) Au–polymer hybrid microgels. The Au–polymer hybrid microgels were also conveniently completed through an anion-exchange reaction and redox reaction. The ILs microgels were added to an aqueous solution of chloroauric acid at room temperature for 12 h. Then, the microgels were immersed into the aqueous solution of sodium borohydride to reduce the chloroauric acid. Then, the Au–polymer hybrid microgels were filtered off, and purified by extensive washing with deionized water several times.

(C) Conductive hybrid microgels. The conductive hybrid microgels were also conveniently obtained through anion-exchange and redox reactions. The ILs microgels were added to an aqueous solution of chloroauric acid at room temperature for 12 h. Then, the microgels were immersed into the solution of pyrrole to obtain a polypyrrole film coating on the surface of the microgels. Then, the conducting polymer hybrid microgels were filtered off, and purified by extensive washing with deionized water several times.

(D) Catalytic microgels. The prepared PIL microgels were added to an aqueous solution of peroxotungstate (POM) at room temperature for 12 h. Then, the microgels were filtered off, washed several times with deionized water, and dried in vacuum to afford PIL microgels loaded with peroxotungstate. The potential of the POM-loaded microgels for catalytic applications was checked as follows: the PIL microgels loaded with POM were dispersed in acetonitrile solution (1 mL) containing cyclooctene (0.2307 g, 2.1 mmol) and hydrogen peroxide (30% aq. solution, 0.0647 g). Then, the reaction mixture was stirred at 333 K for 5 h. After the completion of the reaction, the ILs microgels were separated by filtration, washed with solvent, and dried in vacuum prior to being recycled.

(E) Carbene microspheres. The carbene microspheres were obtained by treatment of the imidazolium-based PIL microgels with NaH in THF at 273 K (*i.e.*, a catalytic amount of DMSO) under N_2 atmosphere.

(F) Carbon particles. The PIL microgels were first immersed in aqueous solution of $FeCl_3$ for 3 h, and then after washing and drying in air the treated microgels were heated under a N_2 atmosphere to 623 K, at a heating rate of 1 K min^{-1}, and then maintained at 623 K for 2 h, and subsequently heated to 1073 K at a heating rate of 1 K min^{-1} and finally placed at 1073 K for 5 h. Then, the resulting carbon particles were taken out and cooled to room temperature.

Acknowledgements

We gratefully acknowledge the financial support from the NSFC (21025311, 21121004, 21261130581, 91027016), Ministry of Education (2011Z01014), MOST (2011CB808403, 2013CB834502) and the transregional project (TRR61).

Notes and references

1 B. R. Saunders and B. Vincent, *Adv. Colloid Interface Sci.*, 1999, **80**, 1.
2 (*a*) Y. Lu, N. Welsch and M. Ballauff, *Chemical Design of Responsive Microgels*, Springer, Berlin, 2011, vol. 234, p.

129; (*b*) L. R. B. Kesselman, S. Shinwary, P. R. Selvaganapathy and T. Hoare, *Small*, 2012, **8**, 1092; (*c*) M. Das, H. Zhang and E. Kumacheva, *Annu. Rev. Mater. Res.*, 2006, **36**, 117; (*d*) D. Parasuraman and M. J. Serpe, *ACS Appl. Mater. Interfaces*, 2011, **3**, 2732; (*e*) A. Wang, Y. Cui, J. Li and J. C. M. van Hest, *Adv. Funct. Mater.*, 2012, **22**, 2673; (*f*) K. Iwai, Y. Matsumura, S. Uchiyamaab and A. P. de Silva, *J. Mater. Chem.*, 2005, **15**, 2796; (*g*) G. Huang and Z. Hu, *Macromolecules*, 2007, **40**, 3749; (*h*) D. Wang, T. Liu, J. Yin and S. Liu, *Macromolecules*, 2011, **44**, 2282.

3 (*a*) R. Contreras-Caceres, S. Abalde-Cela, P. Guardia-Giros, A. Fernandez-Barbero, J. Perez-Juste, R. A. Alvarez-Puebla and L. M. Liz-Marzan, *Langmuir*, 2011, **27**, 4520; (*b*) Y. Lu, J. Yuan, F. Polzer, M. Drechsler and J. Preussner, *ACS Nano*, 2010, **4**, 7078; (*c*) F. Tang, N. Ma, L. Tong, F. He and L. Li, *Langmuir*, 2012, **28**, 883.

4 (*a*) T. Welton, *Chem. Rev.*, 1999, **99**, 2071; (*b*) T. Torimoto, T. Tsuda, K. Okazaki and S. Kuwabata, *Adv. Mater.*, 2010, **22**, 1196.

5 R. D. Rogers and K. R. Seddon, *Science*, 2003, **302**, 792.

6 (*a*) C. H. Lee, H. S. Lim, J. Kim and J. H. Cho, *ACS Nano*, 2011, **5**, 7397; (*b*) M. T. Rahman, Z. Barikbin, A. Z. M. Badruddoza, P. S. Doyle and S. A. Khan, *Langmuir*, 2013, **29**, 9535; (*c*) M. Tokuda, T. Shindo and H. Minami, *Langmuir*, 2013, **29**, 11284; (*d*) H. Gu and J. Texter, *Polymer*, 2014, **55**, 3378.

7 (*a*) S. G. Lee, *Chem. Commun.*, 2006, 1049; (*b*) Z. Fei, T. J. Geldbach, D. Zhao and P. J. Dyson, *Chem.–Eur. J.*, 2006, **12**, 2122.

8 (*a*) Q. Chen, S. C. Bae and S. Granick, *Nature*, 2011, **469**, 381–384; (*b*) Q. Chen, J. K. Whitmer, S. Jiang, S. C. Bae, E. Luijten and S. Granick, *Science*, 2011, **331**, 199–202.

9 (*a*) J. Texter, *Macromol. Rapid Commun.*, 2012, **33**, 1996; (*b*) J. Y. Yuan, D. Mecerreyes and M. Antonietti, *Prog. Polym. Sci.*, 2013, **38**, 1009.

10 (*a*) S. Q. Xu, Z. H. Nie, M. Seo, P. Lewis, E. Kumacheva, H. A. Stone, P. Garstecki, D. B. Weibel, I. Gitlin and G. M. Whitesides, *Angew. Chem., Int. Ed.*, 2005, **44**, 724; (*b*) E. Tumarkin and E. Kumacheva, *Chem. Soc. Rev.*, 2009, **38**, 2161; (*c*) S. Seiffert, *Macromol. Rapid Commun.*, 2011, **32**, 1600; (*d*) Y. J. Zhao, X. W. Zhao, C. Sun, J. Li, R. Zhu and Z. Z. Gu, *Anal. Chem.*, 2008, **80**, 1598.

11 C. Serra, N. Berton, M. Bouquey, L. Prat and G. Hadziioannou, *Langmuir*, 2007, **23**, 7745.

12 (*a*) R. Marcilla, M. S. Paniagua, B. L. Ruiz, E. L. Cabarcos, E. Ochoteco, H. Grande and D. Mecerreyes, *J. Polym. Sci., Part A: Polym. Chem.*, 2006, **44**, 3958; (*b*) R. Marcilla, J. A. Blazquez, R. Fernandez, H. Grande, J. A. Pomposo and D. Mecerreyes, *Macromol. Chem. Phys.*, 2005, **206**, 299.

13 (*a*) E. Bianchi, R. Blaak and C. N. Likos, *Phys. Chem. Chem. Phys.*, 2011, **13**, 6397; (*b*) A. B. Pawar and I. Kretzschmar, *Macromol. Rapid Commun.*, 2010, **31**, 150.

14 (*a*) T. Kaufmann, M. T. Gokmen, C. Wendeln, M. Schneiders, S. Rinnen, H. F. Arlinghaus, S. A. F. Bon, F. E. Du Prez and B. J. Ravoo, *Adv. Mater.*, 2011, **23**, 79; (*b*) J. Cui, W. Zhu, N. Gao, J. Li, H. Yang, Y. Jiang, P. Seidel, B. J. Ravoo and G. Li, *Angew. Chem., Int. Ed.*, 2014, **53**, 3844.

15 H. S. Schrekker, M. A. Gelesky, M. P. Stracke, C. M. L. Schrekker, G. Machado, S. R. Teixeira, J. C. Rubim and J. Dupont, *J. Colloid Interface Sci.*, 2007, **316**, 189.

16 D. L. Long, R. Tsunashima and L. Cronin, *Angew. Chem., Int. Ed.*, 2010, **49**, 1736.

17 K. Yamaguchi, C. Yoshida, S. Uchida and N. Mizuno, *J. Am. Chem. Soc.*, 2005, **127**, 530.

18 C. Rocchiccioli-Deltcheff, M. Fournier, R. Frank and R. Thouvenot, *Inorg. Chem.*, 1983, **22**, 207.

19 (*a*) A. Grossmann and D. Enders, *Angew. Chem., Int. Ed.*, 2012, **51**, 314; (*b*) V. Nair, S. Bindu and V. Sreekumar, *Angew. Chem., Int. Ed*, 2004, **43**, 5130; (*c*) A. J. Arduengo III, R. L. Harlow and M. K. Kline, *J. Am. Chem. Soc.*, 1991, **113**, 361; (*d*) A. J. Arduengo III, J. R. Goerlich and W. J. Marshall, *J. Am. Chem. Soc.*, 1995, **117**, 11027; (*e*) A. J. Arduengo III, R. Krafczyk and R. Schmutzler, *Tetrahedron*, 1999, **55**, 14523.

20 H. Zhou, W. Z. Zhang, Y. M. Wang, J. P. Qu and X. B. Lu, *Macromolecules*, 2009, **42**, 5419.

21 J. Jang and J. Bae, *Angew. Chem., Int. Ed.*, 2004, **43**, 3803.

22 W. X. Zhang, J. C. Cui, C. A. Tao, C. X. Lin, Y. G. Wu and G. T. Li, *Langmuir*, 2009, **25**, 8235.

23 C. Zhao, H. Z. Wang, N. Yan, C. X. Xiao, X. D. Mu, P. J. Dyson and Y. Kou, *J. Catal.*, 2007, **250**, 33.